An Open-Source Multiscale Framework for the Simulation of Nanoscale Devices

Samantha Bruzzone, Giuseppe Iannaccone, Nicola Marzari, and Gianluca Fiori

***Abstract*— We present a general simulation framework for assessing the performance of nanoscale devices that combines several powerful and widely used open-source codes, and based on minimal but chemically accurate tight-binding Hamiltonians obtained from density-functional theory calculations and using maximally localized Wannier functions to represent the electronic state. Transport properties are then computed within the nonequilibrium Green's function formalism. We illustrate the capabilities of this framework applying it to a transistor with generic gate geometries, i.e., a double-gate nanoscale field-effect transistor where the channel is formed by graphene nanoribbons terminated with hydrogen, fluorine, and OH groups.**

***Index Terms*— *Ab-initio*, DFT, multi-scale, NEGF, transistors.**

I. Introduction

RESEARCH in electronic devices is exploring an ever broader spectrum of suitable materials to overcome the challenges of improving performance even when device sizes are scaled down to only a few nanometers. In addition, in their attempts at tuning and optimizing material properties for nanoelectronics, researchers use techniques such as chemical functionalizations, nanoscale patterning, or mechanical strains that further enlarge the effective materials design space.

The electronic properties of most novel materials are not as well known as those of conventional semiconductors, but could be obtained in accurate and cost-effective ways with quantum mechanical simulations.

The need for multiscale simulations becomes then apparent [1]; on the one hand, researchers need detailed *ab-initio* simulation tools for computing electronic properties and on the other hand, the electrical simulation of complete devices with thousands of atoms requires descriptions at a higher level of abstraction. Recently, given the reduced device size and the impact of single atoms and localized defects on device operation, atomistic simulation methods have gained acceptance for the latter task. "Atomistic" means that atoms are individually represented in the physical description, typically through sparse tight-binding (TB) Hamiltonians suitable for the computation of transport properties by means of the nonequilibrium Green's functions (NEGFs) formalism.

The success of TB descriptions is due to their high degree of scalability and adaptability, meaning that the choice of both the size of the basis set and of the approximations can be tailored to the system considered and the properties investigated, ranging from fully empirical calculations (suitable for systems up to one million atoms) to fully *ab-initio* (which can be realistically used for systems of up to few hundred atoms).

A multiscale approach is typically implemented by computing the electronic properties and the Hamiltonian of the material under investigation using density-functional theory methods, and then by extracting a relatively sparse TB Hamiltonian from a fitting procedure [2]–[5]. This often leads to nontrivial problems related to the choice of the proper structure of the TB Hamiltonian and to the lack of generality of the results obtained.

It would be preferable to obtain the matrix elements from first principles, starting from the knowledge of the localized basis set. A full treatment of the *ab-initio* problem on a periodic system based on local orbitals has been developed both in the full Hartree–Fock [6] and DFT [7]–[9] descriptions, providing some advantages with respect to plane wave approaches, depending on the desired property, and some challenges mainly due to the incompleteness of the basis set.

In this paper, we apply an *ab-initio* TB multiscale method based on DFT and NEGF formalism [10]–[12] to evaluate the performance of field effect transistors (FETs) based on novel material [13]. In particular, our framework relies on the computation of the Hamiltonian of the material considered with density-functional theory calculations, and on the transformation from a Bloch base of extended eigenstates onto a basis of maximally localized Wannier functions (MLWFs), centered on the actual positions of atoms or bonds in the crystal [14]–[17], exploiting available open-source codes like Quantum Espresso and Wannier90 [18], [19]. The TB Hamiltonian obtained has then been included in the open-source code NanoTCAD ViDES [20], where realistic gate geometries and architectures can be considered. As a case study, we have focused our attention on functionalized graphene nanoribbon transistors.

II. Methods and Computational Details

The goal is to find a TB representation of the Hamiltonian H of the system under investigation to study transport with

Manuscript received July 11, 2013; revised September 27, 2013; accepted November 15, 2013. Date of publication December 5, 2013; date of current version December 20, 2013. This work was supported in part by the EC 7FP through the Project GRADE under Contract 317839 and in part by the Project GO-NEXTs under Contract 309201. The review of this paper was arranged by Editor A. Schenk.

S. Bruzzone, G. Iannaccone, and G. Fiori are with the Dipartimento Ingegneria dell'Informazione, University of Pisa, Pisa 56122, Italy (e-mail: samantha.bruzzone@gmail.com; giuseppe.iannaccone@unipi.it; g.fiori@iet.unipi.it).

N. Marzari is with the Theory and Simulation of Materials Laboratory, École Polytechnique Fédérale de Lausanne, Lausanne 1015, Switzerland (e-mail: nicola.marzari@epfl.ch).

Color versions of one or more of the figures in this paper are available online at http://ieeexplore.ieee.org.

Digital Object Identifier 10.1109/TED.2013.2291909

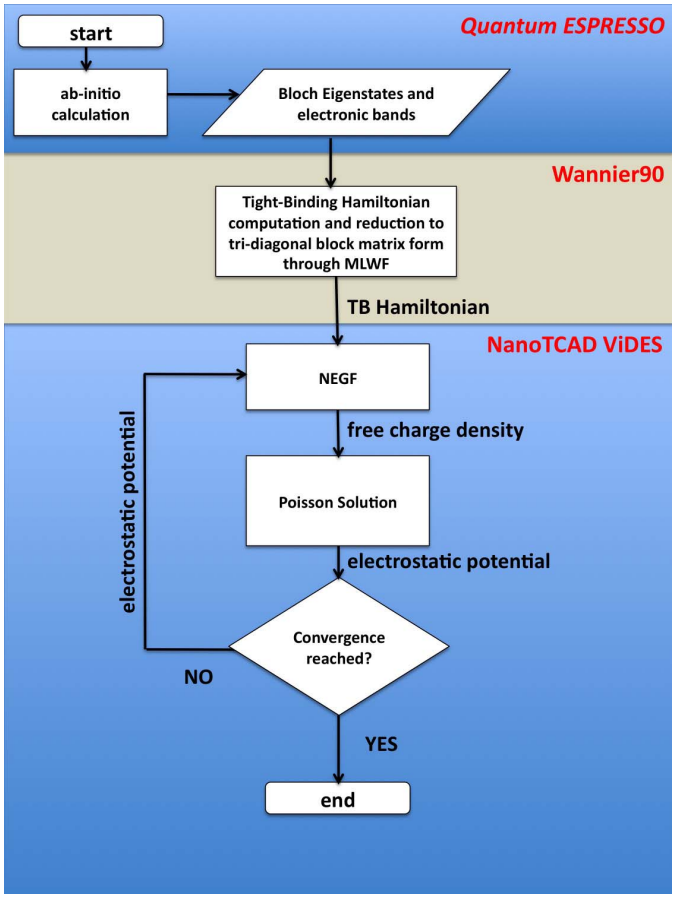

Fig. 1. Flowchart of the proposed procedure.

the NEGF formalism. The Wannier representation [21]–[23], essentially a real-space picture of localized orbitals, can ideally describe the electronic and dielectric properties of materials; it represents the solid-state equivalent of "localized molecular orbitals" [24]–[26] and offers a reliable picture of phenomena, such as chemical bonding, where electron spatial localization plays an important role. The change of representations between Bloch and Wannier basis sets is obtained through unitary matrices, not uniquely defined, where different choices lead to different spatial localizations of Wannier functions. The key point is to find an appropriate transformation, which allows the more pronounced localization, i.e., the so-called MLWFs [27], [28]. Such an assumption is of primary importance to reduce the Hamiltonian dimensions and eventually the computational cost.

A flow diagram of the proposed multiscale approach is shown in Fig. 1. As can be seen, three different simulation tools are exploited: 1) Quantum Espresso [18]; 2) Wannier90 [19]; and 3) NanoTCAD ViDES [20]. They are all available as open-source codes; in addition, many other open source or publicly available quantum simulation codes could be used in lieu of Quantum ESPRESSO, and are directly interfaced with Wannier90. Some of these include VASP, Abinit, CASTEP, Wien2K, FLEUR, Siesta, and so on.

The procedure starts from the construction of the matrix elements of the Hamiltonian in a Wannier functions basis set. The atomic structure must be optimized first, and for this optimal geometry, the electronic bands are transformed into an alternative representation based on MLWFs, using Wannier90. In particular, following [27], a set of Wannier functions is defined in terms of the Bloch eigenstates $\psi_{n\mathbf{k}}$ through the unitary transformation

$$w_{n\mathbf{R}}(\mathbf{r}) = \frac{V}{(2\pi)^3}\int_{\mathrm{BZ}} e^{-\imath\mathbf{k}\cdot\mathbf{R}}\psi_{n\mathbf{k}}(\mathbf{r})\,\mathbf{dk} \tag{1}$$

where V is the real-space unit cell volume of the crystal, k is the wave vector, BZ is the Brillouin zone over which the integral is performed, $\mathbf{R}$ is Bravais lattice vector, and n is the band index.

The phases of the Bloch functions $\psi_{n\mathbf{k}} = e^{\imath\mathbf{k}\cdot\mathbf{r}}u_{n\mathbf{k}}$ coming out of the electronic structure codes are arbitrary, but the phase term affects the shape and spatial extent, such as the spread of Wannier functions. For the case of an isolated group of bands, the gauge freedoms allowed are more general, and involve not only a phase, but entire unitary transformations between all the bands at every point in reciprocal space

$$u_{n\mathbf{k}} = \sum_{m=1}^{N} U_{mn}^{(\mathbf{k})}u_{m\mathbf{k}} \tag{2}$$

where $U^{\mathbf{k}}$ is a unitary matrix mixing the bands at wave vector $\mathbf{k}$. The resulting functions can be called "generalized Wannier functions," but are not in general localized or chemically meaningful. Localization can be enforced by solving a problem of functional minimization in the space of the matrices $U^{(\mathbf{k})}$. In [27], the functional

$$\Omega = \sum_{m}\left[\left\langle r^2\right\rangle_n - \overline{\mathbf{r}}_n^2\right] \tag{3}$$

is introduced as a measure of the spread of the Wannier functions in analogy with Boys' definition of localized molecular orbitals [24], [27]. When minimizing Ohm with respect to the unitary transformations $U^{(\mathbf{k})}$, the resulting WF will be maximally localized (and also real valued, apart from an arbitrary overall phase factor).

In this case, Wannier functions are built to ensure that WF centers correspond to atomic sites, even if in general the WFs can sit offsite (e.g., in the center of a bond). So, here each Hamiltonian element represents the interaction between the two atomic sites on which the WF are localized. In this basis, the element (n, m) of the Hamiltonian matrix reads

$$H\left(\mathbf{R}_j - \mathbf{R}_i\right)_{nm} = \left\langle w_{n\mathbf{R}_i}\left|H\right|w_{m\mathbf{R}_j}\right\rangle \tag{4}$$

and represents the interaction between the nth Wannier function of cell i with the mth Wannier function of cell j.

In particular, if N_A is the number of atoms in the elementary cell, and the channel is composed by N_C unit cells, the Hamiltonian is composed by $N_C \times N_C$ block matrices of order N_A. $H\left(\mathbf{R}_j - \mathbf{R}_i\right)$ then represents the coupling matrix between the cell i and the cell j, as shown in Fig. 2, the smaller the coupling between cells, the smaller the number of nonzero elements of H and then the faster the transport computation [29]. The limiting case is represented by a coupling between nearest neighbor cells (i.e., i and $i+1$ and i and $i-1$ cells), so that H reduces to a tridiagonal block matrix.

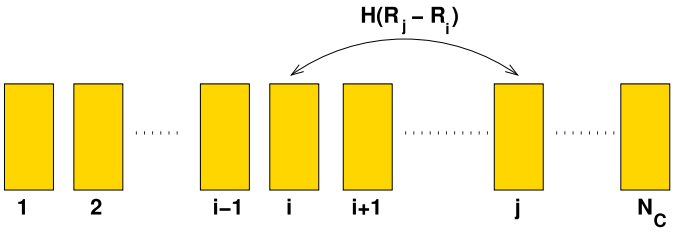

Fig. 2. Illustration of the coupling between the unit cells composing the system considered. N_C is the total number of cells.

From a numerical point of view, the calculation of the Bloch functions on a mesh of **k** points has been performed by means of the plane-wave DFT code PWSCF, within the Quantum ESPRESSO distribution [18]. All DFT calculations were carried out within the PBE generalized gradient approximation and using ultrasoft Rabe-Rappe-Kaxiras-Joannopoulos pseudopotentials to represent ionic cores. The cutoff used for energy and density was 40 and 480 Ry, respectively, and the Brillouin zone was sampled with a $1 \times 1 \times 1 \times 16$ Monkhorst-Pack grid. The geometries of all the considered ribbons have been optimized by relaxing the atomic positions until all components of all forces become smaller than 10^{-4} Ry/au. The same distance, equal to 24 Å, separates the ribbon periodic replica in the two directions, perpendicular and parallel to the ribbon plane.

Once the Hamiltonian has been obtained, the transport problem is solved through the solution of the Green's function

$$G(E) = \left[ES - H - \Sigma_S - \Sigma_D - \Sigma_{ph}\right]^{-1} \tag{5}$$

where E is the energy, S is the overlap matrix, which eventually reduces to the identity matrix in case of an orthogonal basis set [30], Σ_S and Σ_D are the self-energies of the source and drain, respectively. In addition, electron-phonon interactions can be considered through the definition of Σ_{ph}, which has not been considered in this paper (see [31]).

If H is a tridiagonal block matrix, the most efficient algorithm is represented by the recursive Green's function method [32], whose complexity is $O(N_C N_A^3)$. Also the numerical solution of the self-energy deserves attention, since it can affect the overall performance. In our case, we have adopted a closed-form expression based on the algebra derived in [33] and [34], which provides faster results than the transfer Hamiltonian formalism proposed in [35].

From the computed $G(E)$, it is possible to obtain all the relevant quantities, such as free charge concentration $\rho_{\text{free}}(\vec{r})$ in correspondence of each atom of the system under investigation, the transmission coefficients, and consequently the current flowing in the device. Details can be found in [36].

Charge density computation can then be included in a self-consistent scheme solving the Poisson equation, in order to feed the transport problem with the potential obtained through

$$\nabla\left[\epsilon(\vec{r})\nabla\phi(\vec{r})\right] = -q\left[\rho_{\text{free}}(\vec{r}) + \rho_{\text{fix}}\right] \tag{6}$$

where $\phi(\vec{r})$ is the electrostatic potential, q is the electron charge, $\epsilon(\vec{r})$ is the dielectric constant, and ρ_{fix} is the fixed charge.

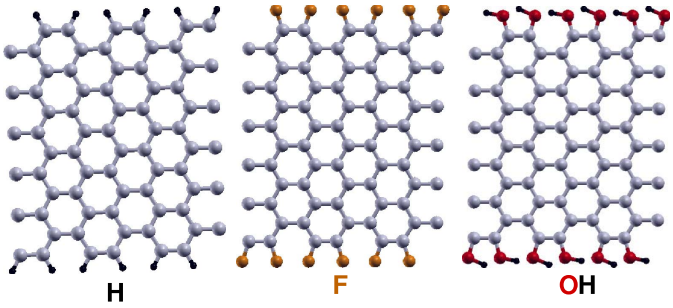

Fig. 3. Atomistic structure of AGNR-12 with different edge chemistry. Three unit cells are shown for each type of GNR.

In particular, the nonlinear system is solved with the Newton/Raphson method within a Gummel iterative scheme [37]. The self-consistent scheme is implemented in the NanoTCAD ViDES code.

III. Results and Discussion

To verify the implemented multiscale approach, we have focused on edge-functionalized armchair graphene nanoribbon, and in particular on H:AGNR-12, F:AGRN-12, and OH:AGNR-12 [38], [39]. The optimized structures are shown in Fig. 3.

For each nanoribbon, we have calculated the electronic band structure according to DFT. The geometric and electronic band structure of H and F:AGNR-12 are in agreement with results presented in [38], while our optimization of OH:AGNR-12 has shown the presence of predictable hydrogen bonds between the oxygens, which is not considered in [38], but affects only slightly the band structure.

Attention has to be posed on the choice of starting guess for the localized orbitals onto which the Bloch states have to be projected. For the considered materials, conduction and valence bands have π symmetry, so p_z orbitals have been considered.

The calculated MLWF by means of Wannier90 from the π occupied and unoccupied manifolds of the three nanoribbons map these bands onto an explicit TB basis of localized orbitals, built on one p_z for every C and for every heteroatom [40].

In Fig. 4, we show the bands computed through DFT calculations and by means of the MLWF. As can be seen, the agreements between the two different methods are excellent. In the considered cases, an interaction up to the sixth nearest neighbor cell has been considered.

We have then performed a transport simulation of the graphene nanoribbon FET shown in Fig. 5, where the longitudinal cross section is shown in the inset. The gate is 10-nm long, and a top and bottom metallic gates have been considered. The oxide thickness is equal to 1 nm with a relative dielectric constant $\varepsilon_r = 3.9$. Semi-infinite leads have been considered at both nanoribbon ends. However, we would like to underline that the proposed simulation framework is generic, and metallic contacts, as well as atomistic representation of the oxide could have been considered as well.

To simplify and accelerate computation, in the transport simulation a simplified Hamiltonian has been considered,

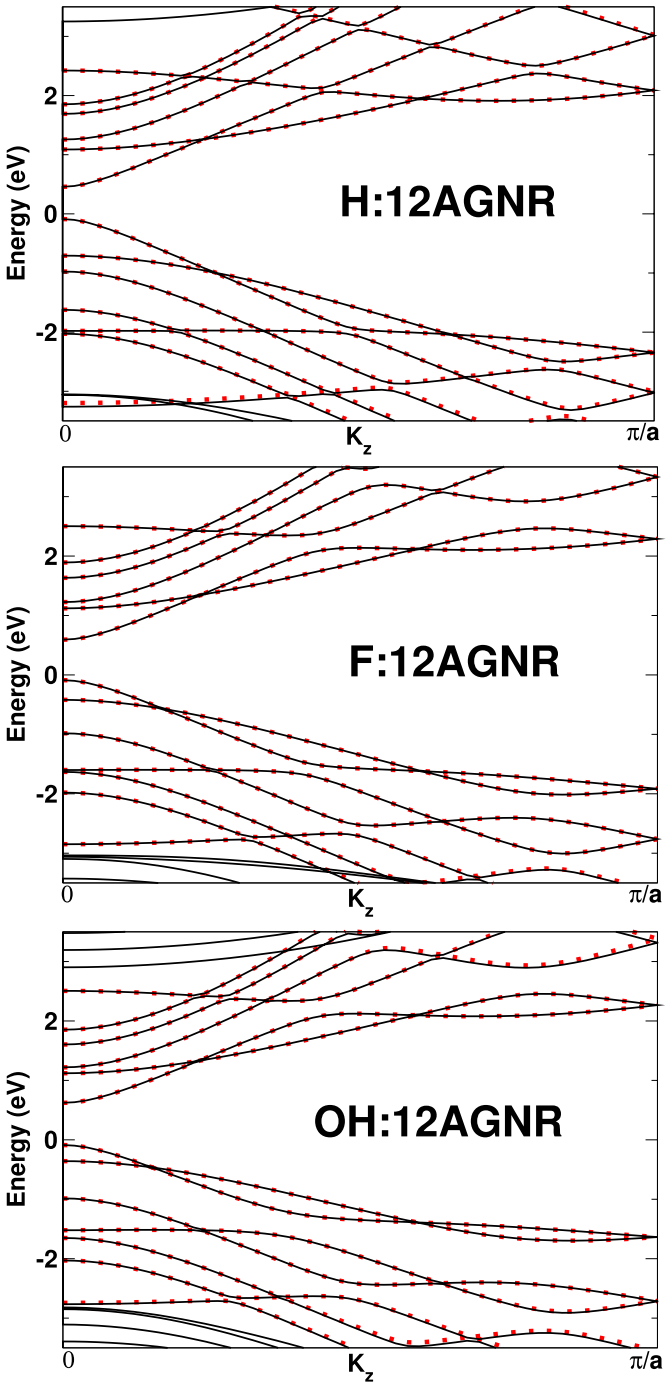

Fig. 4. Band structure (solid black line) and its MLWF interpolation (red dots) for H:AGNR-12, F:AGNR-12, and OH:AGNR-12 obtained by including all p_z MLWF.

where all parameters beyond those related to first neighbor cells are set to zero. This approximation is still accurate, as can be seen in Fig. 6(a), where the transmission coefficient as a function of energy is shown considering all the complete Hamiltonian (black line) and only first neighbor cell interactions (red line). As can be seen, the agreement is good, especially in correspondence of the conduction and valence band edges, i.e., the energy values at which the transmission coefficient becomes equal to 1, which are the most important from the transport point of view.

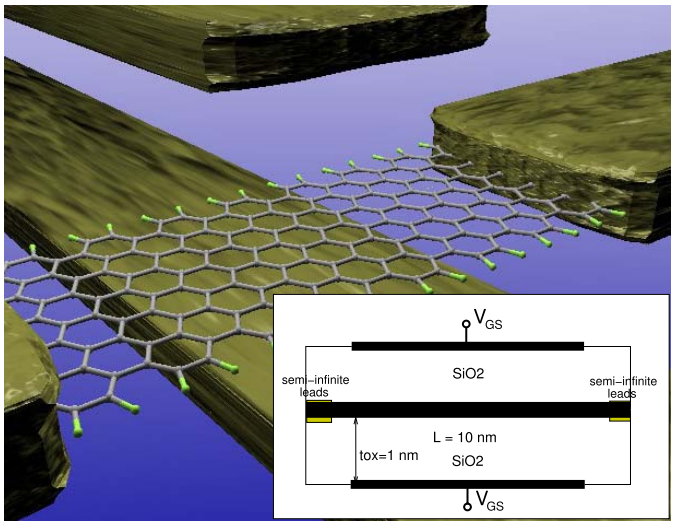

Fig. 5. Sketch of the graphene nanoribbon FET considered in the simulation. The channel is composed by a F:AGNR-12. The gate length is 10 nm, and top and bottom oxide thickness are equal to 1 nm.

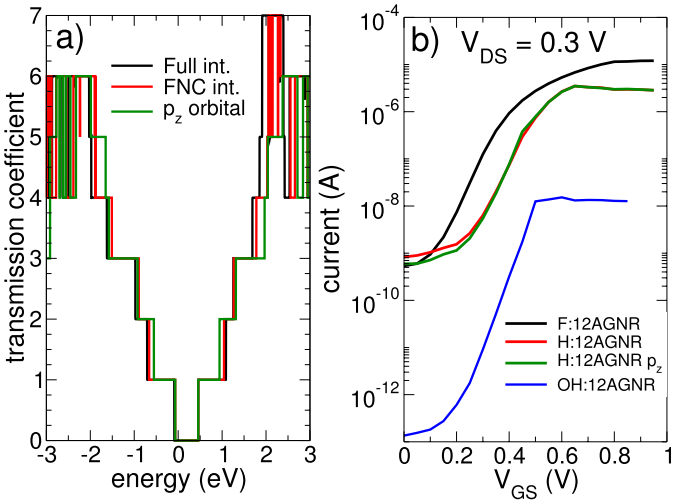

Fig. 6. (a) Transmission coefficient for different V_{GS} and $V_{DS} = 0.3$ V obtained with the full Hamiltonian (black line), with a simplified Hamiltonian considering only first neighbor cell interactions (red line), and with a Hamiltonian with only p_z orbitals. (b) Transfer characteristics for $V_{DS} = 0.3$ V of the considered transistor with different nanoribbon channel.

In Fig. 6(b), the transfer characteristics for a drain-to-source voltage (V_{DS}) equal to 0.3 V are shown for all the three considered materials. The current is modulated over four orders of magnitude and large ON-current can be obtained (order of μA) even with reduced V_{DS}.

By means of the considered approach, we can also evaluate the validity of the simple p_z single orbital semiempirical TB approximations, widely used in the device simulation community. To this purpose, a TB Hamiltonian as in [8] has been considered, taking into account energy relaxation at the GNR edges. In particular, a hopping parameters equal to $t_p = -2.3445$ eV has been considered between carbon atoms, except that in correspondence of atoms at the edges, where $t_p = -2.626$ eV has been assumed. As can be

seen in Fig. 6(a), using the abovementioned parameters, the transmission coefficient (green line) is in a good agreement with the results obtained from MLWF approach, especially in correspondence of the lower 1-D subbands.

In Fig. 6(b) instead the transfer characteristics for the H:12AGNR device, computed by means of the p_z orbital Hamiltonian are shown. As can be noted, they are in really a good agreement with the transfer characteristics computed through the more accurate MLWF Hamiltonian.

IV. Conclusion

We have presented a multiscale simulation framework suitable for the performance assessment of nanoelectronic devices. The framework is based on three open codes dealing with the calculation of basic properties of the materials through *ab-initio* methods (Quantum Espresso), self-extraction of a TB like Hamiltonian by means of transformation in the MLWF representation (Wannier90), and the self-consistent solution of 1-D/2-D/3-D Poisson and transport equation in nanoscale devices with realistic architectures (NanoTCAD ViDES).

The framework is very general, and therefore provides a tangible advantage with respect to semiempirical TB methods, which often need to be customized for each material and/or simulation objective.

References

[1] G. Fiori and G. Iannaccone, "Multiscale modeling for graphene-based nanoscale transistors," *Proc. IEEE*, vol. 101, no. 7, pp. 1653–1669, Jul. 2013.

[2] A. V. Podolskiy and P. Vogl, "Compact expression for the angular dependence of tight-binding Hamiltonian matrix elements," *Phys. Rev. B*, vol. 69, no. 23, pp. 233101-1–233101-5, Jun. 2004.

[3] T. B. Boykin, G. Klimeck, and F. Oyafuso, "Valence band effective-mass expressions in the $sp^3d^5s^*$ empirical tight-binding model applied to a Si and Ge parametrization," *Phys. Rev. B*, vol. 69, pp. 115201-1–115201-10, Mar. 2004.

[4] G. Fiori, S. Lebègue, A. Betti, P. Michetti, M. Klintenberg, O. Eriksson, *et al.*, "Simulation of hydrogenated graphene field-effect transistors through a multiscale approach," *Phys. Rev. B*, vol. 82, no. 15, pp. 153404-1–153404-4, 2010.

[5] G. Fiori, A. Betti, S. Bruzzone, and G. Iannaccone, "Lateral graphene-hBCN heterostructures as a platform for fully two-dimensional transistors," *ACS Nano*, vol. 6, no. 3, pp. 2642–2648, 2012.

[6] E. Artacho and F. Ynduráin, "Nonparametrized tight-binding method for local and extended defects in homopolar semiconductors," *Phys. Rev. B*, vol. 44, pp. 6169–6187, Sep. 1991.

[7] O. F. Sankey and D. J. Niklewski, "*Ab initio* multicenter tight-binding model for molecular-dynamics simulations and other applications in covalent systems," *Phys. Rev. B*, vol. 40, pp. 3979–3995, Aug. 1989.

[8] R. E. Cohen, M. J. Mehl, and D. A. Papaconstantopoulos, "Tight-binding total-energy method for transition and noble metals," *Phys. Rev. B*, vol. 50, pp. 14694–14697, Nov. 1994.

[9] P. Ordejón, E. Artacho, and J. M. Soler, "Self-consistent order-*n* density-functional calculations for very large systems," *Phys. Rev. B*, vol. 53, pp. R10441–R10444, Apr. 1996.

[10] A. R. Rocha, V. M. Garcia-Suarez, S. Bailey, C. Lambert, J. Ferrer, and S. Sanvito, "Spin and molecular electronics in atomically generated orbital landscapes," *Phys. Rev. B*, vol. 73, no. 8, pp. 085414-1–085414-22, Feb. 2006.

[11] K. Stokbro, J. Taylor, M. Brandbyge, and P. Ordejon, "TranSIESTA: A spice for molecular electronics," *Ann. New York Acad. Sci.*, vol. 106, no. 1, pp. 212–226, 2003.

[12] A. Di Carlo, A. Pecchia, L. Latessa, T. Frauenheim, and G. Seifert, "Tight-binding DFT for molecular electronics (gDFTB)," in *Introducing Molecular Electronics*, vol. 680. G. Cuniberti, K. Richter, and G. Fagas, Eds. New York, NY, USA: Springer, 2005, pp. 153–184.

[13] J. Chang, L. F. Register, and S. K. Banerjee, "Topological insulator Bi_2Se_3 thin films as an alternative channel material in metal-oxide-semiconductor field-effect transistors," *J. Appl. Phys.*, vol. 112, no. 12, pp. 124511-1–124511-5, 2012.

[14] A. Calzolari, N. Marzari, I. Souza, and M. Buongiorno Nardelli, "*Ab initio* transport properties of nanostructures from maximally localized Wannier functions," *Phys. Rev. B*, vol. 69, pp. 035108-1–035108-10, Jan. 2004.

[15] Y.-S. Lee, M. B. Nardelli, and N. Marzari, "Band structure and quantum conductance of nanostructures from maximally localized Wannier functions: The case of functionalized carbon nanotubes," *Phys. Rev. Lett.*, vol. 95, pp. 076804-1–076804-4, Aug. 2005.

[16] M. Strange, I. S. Kristensen, K. S. Thygesen, and K. W. Jacobsen, "Benchmark density functional theory calculations for nanoscale conductance," *J. Chem. Phys.*, vol. 128, no. 11, pp. 1–6, 2008.

[17] H. Lin, J. Rauba, K. Thygesen, K. Jacobsen, M. Simmons, and W. Hofer, "English first-principles modelling of scanning tunneling microscopy using non-equilibrium Green's functions," *Frontier. Phys. China*, vol. 5, no. 4, pp. 369–379, 2010.

[18] P. Giannozzi, S. Baroni, N. Bonini, M. Calandra, R. Car, C. Cavazzoni, *et al.*, "Quantum espresso: A modular and open-source software project for quantum simulations of materials," *J. Phys., Condensed Matter*, vol. 21, no. 39, pp. 395502-1–395502-3, 2009.

[19] A. A. Mostofi, J. R. Yates, Y.-S. Lee, I. Souza, D. Vanderbilt, and N. Marzari, "Wannier90: A tool for obtaining maximally-localised Wannier functions," *Comput. Phys. Commun.*, vol. 178, no. 9, pp. 685–699, 2008.

[20] G. Fiori and G. Iannaccone, "Multiscale modeling for graphene-based nanoscale transistors," *Proc. IEEE*, vol. 101, no. 7, pp. 1653–1669, Jul. 2013.

[21] G. H. Wannier, "The structure of electronic excitation levels in insulating crystals," *Phys. Rev.*, vol. 52, pp. 191–197, Aug. 1937.

[22] W. Kohn, "Analytic properties of Bloch waves and Wannier functions," *Phys. Rev.*, vol. 115, pp. 809–821, Aug. 1959.

[23] J. D. Cloizeaux, "Orthogonal orbitals and generalized Wannier functions," *Phys. Rev.*, vol. 129, pp. 554–566, Jan. 1963.

[24] S. F. Boys, "Construction of some molecular orbitals to be approximately invariant for changes from one molecule to another," *Rev. Model Phys.*, vol. 32, pp. 296–299, Apr. 1960.

[25] J. M. Foster and S. F. Boys, "Canonical configurational interaction procedure," *Rev. Model Phys.*, vol. 32, pp. 300–302, Apr. 1960.

[26] J. M. Foster and S. F. Boys, "A quantum variational calculation for HCHO," *Rev. Mod. Phys.*, vol. 32, pp. 303–304, Apr. 1960.

[27] N. Marzari and D. Vanderbilt, "Maximally localized generalized Wannier functions for composite energy bands," *Phys. Rev. B*, vol. 56, pp. 12847–12865, Nov. 1997.

[28] N. Marzari, A. A. Mostofi, J. R. Yates, I. Souza, and D. Vanderbilt, "Maximally localized Wannier functions: Theory and applications," *Rev. Model Phys.*, vol. 84, pp. 1419–1475, Oct. 2012.

[29] M. Shelley, N. Poilvert, A. A. Mostofi, and N. Marzari, "Automated quantum conductance calculations using maximally-localised Wannier functions," *Comput. Phys. Commun.*, vol. 182, no. 10, pp. 2174–2183, 2011.

[30] A. Ferretti, A. Calzolari, B. Bonferroni, and R. D. Felice, "Maximally localized Wannier functions constructed from projector-augmented waves or ultrasoft pseudopotentials," *J. Phys., Condensed Matter*, vol. 19, no. 3, pp. 036215-1–036215-3, 2007.

[31] S. Kim and N. Marzari, "First-principles quantum transport with electron-vibration interactions: A maximally localized Wannier functions approach," *Phys. Rev. B*, vol. 87, no. 24, pp. 245407-1–245407-11, Jun. 2013.

[32] R. Lake, G. Klimeck, R. C. Bowen, and D. Jovanovic, "Single and multi-band modeling of quantum electron transport through layered semiconductors devices," *J. Appl. Phys.*, vol. 81, no. 12, pp. 7845–7869, 1997.

[33] M. Luisier, A. Schenk, W. Fichtner, and G. Klimeck, "Atomistic simulation of nanowires in the $sp^3d^5s^*$ tight-binding formalism: From boundary conditions to strain calculations," *Phys. Rev. B*, vol. 74, pp. 205323-1-205323–3, Jan. 2006.

[34] M. Wimmer, "Quantum transport in nanosctructures: From computational concepts to spintronics in graphene and magnetic tunnel junctions," Ph.D. dissertation, Dept. Math., Univ. Regensburg, Regensburg, Germany, 2009.

[35] M. L. Sancho, J. M. L. Sancho, and J. Rubio, "Highly convergent schemes for the calculation of bulk and surface green function," *J. Phys. F, Metal Phys.*, vol. 15, no. 4, pp. 851–858, 1984.

[36] G. Fiori, G. Iannaccone, and G. Klimeck, "A three-dimensional simulation study of the performance of carbon nanotube field-effect transistors with doped reservoirs and realistic geometry," *IEEE Trans. Electron Devices*, vol. 53, no. 8, pp. 1782–1788, Aug. 2006.

[37] A. Trellakis, A. Galick, A. Pacelli, and U. Ravaioli, "Iteration scheme for the solution of the two-dimensional Schrödinger-Poisson equations in quantum structures," *J. Appl. Phys.*, vol. 81, no. 1, pp. 7880–7884, 1997.

[38] Y. Ouyang, Y. Yoon, and J. Guo, "Edge chemistry engineering of graphene nanoribbon transistors: A computational study," in *Proc. IEEE IEDM*, Dec. 2008, pp. 1–4.

[39] N. Rosenkranz, C. Till, C. Thomsen, and J. Maultzsch, "*Ab initio* calculations of edge-functionalized armchair graphene nanoribbons: Structural, electronic, and vibrational effects," *Phys. Rev. B*, vol. 84, pp. 195438-1–195438-7, Nov. 2011.

[40] G. Cantele, Y.-S. Lee, D. Ninno, and N. Marzari, "Spin channels in functionalized graphene nanoribbons," *Nano Lett.*, vol. 9, no. 10, pp. 3425–3429, 2009.

Authors' photographs and biographies not available at the time of publication.